International Journal of Food Studies | IJFS April 2023 | Volume 12 | pages 95–111

Experimental Study and Modelling of the Sublimation and Desorption Periods for Freeze Drying of Apple, Banana and Strawberry

Víctor A. Reale[a], Ricardo M. Torrez Irigoyen[a,b*], and Sergio A. Giner[a,b,c]

[a] Centro de Investigación y Desarrollo en Criotecnología de Alimentos (CIDCA). Facultad de Ciencias Exactas, Universidad Nacional de La Plata, Calle 47 y 116 (1900)- La Plata, Provincia de Buenos Aires, Argentina.
[b] Facultad de Ingeniería, Universidad Nacional de La Plata.
[c] Comisión de Investigaciones Científicas de la Provincia de Buenos Aires, Argentina.
[*]Corresponding author
ricardo_mart2@yahoo.com.ar
Tel: +549 221 4249287

Received: 9 March 2022; Published online: 18 April 2023

Abstract

Slices of fresh apple, banana and strawberry were frozen at -20 ^{o}C and freeze-dried using a shelf temperature of 40 ^{o}C. Theoretical expressions were proposed to predict vapor transfer kinetics during the primary and secondary drying stages. In the former, a model that predicts the sublimation rate as a function of time, considering the increasing dried layer thickness, was used, which improves greatly the sublimation time equation offered in several textbooks without adding much complexity. In the latter, an analytical solution of the unsteady state diffusion equation was applied. Permeabilities were determined for the primary drying model at an absolute pressure of about 30 Pa, though the relevant kinetic coefficient combines permeability and the mass of ice to sublime relative to the dry matter (sublimation kinetic coefficient). In the secondary drying stage, diffusion coefficients of vapor in the dried layer were in the order of 10^{-09} m^2 s^{-1} for pressures of about 3-5 Pa. In both periods, agreement of predicted and experimental values was more than satisfactory. A minimum freeze-drying time of 12, 6.8 and 8.7 h, considering a final moisture content of 4% w/w, was calculated for apple, banana and strawberry, respectively. Normalized drying curves showed a faster sublimation rate for banana, intermediate for strawberry and slowest for apple. On the other hand, desorption curves showed a faster desorption rate for apple, intermediate for banana and slower for strawberry. In each period, the ordering of the relevant kinetic coefficients (sublimation and diffusion coefficients, respectively) represented the ordering of experimental curves.

Keywords: Freeze-drying; Mathematical-model; Apple; Banana; Strawberry

1 Introduction

Freeze-drying is a physicochemical process in which water is removed from a previously frozen product by sublimation of ice during the primary drying stage, and then by desorption of the unfrozen water during the secondary period (García-Amezquita et al., 2016).

Freeze-dried products are considered of the highest quality amongst dehydrated foods due to their higher retention of bioactive compounds; besides, as they do not shrink considerably, the structure is preserved. Freeze-drying is more expensive: the process demands longer drying times with higher energy consumption, so this technique is suitable for highly value-added prod-

 10.7455/ijfs/12.1.2023.a7

Nomenclature

b	Dried layer permeability to the vapor flux, [kg $_{water}$ (m Pa s) $^{-1}$]
C_{2m}	Parameter defined in Equation (15), [m Pa kg $_{water}{}^{-1}$]
D	Water vapor diffusion coefficient in the dried layer, [m^2 s^{-1}]
F_{ice}	Frozen water fraction in the sample, [kg $_{ice}$ kg $_{initialwater}{}^{-1}$]
G	Sublimation rate per unit area in the primary drying period [kg $_{water}$ $m^{-2}s^{-1}$]
K_g	Mass transfer coefficient between sample top surface and condenser, [kg $_{water}$ (m^2Pa s) $^{-1}$]
K_s	Sublimation kinetic coefficient, [s^{-1}]
L	Thickness of material, [m]
m	Moisture content (average in sample) at time t, [kg $_{water}$ kg $_{drymatter}{}^{-1}$]
m_0	Initial moisture content, [kg $_{water}$ kg $_{drymatter}{}^{-1}$]
m_e	Final moisture content for the primary drying period, [kg $_{water}$ kg $_{drymatter}{}^{-1}$]
m_l	Local moisture content at time t, in the desorption period, [kg $_{water}$ kg $_{drymatter}{}^{-1}$]
m_{eq}	Equilibrium moisture content, [kg $_{water}$ kg $_{drymatter}{}^{-1}$]
m_{dd}	Dimensionless mean moisture content
P_{iw}	Vapor pressure of ice in the sublimation front, [Pa]
P_{sw}	Vapor pressure at the surface of the dried layer, [Pa]
P_{aw}	Vapor pressure at the condenser surface, [Pa]
P_w	Pressure at the solid-vapor interface, [Pa]
T_{lp}	Shelf temperature, [K]
T_i	Temperature of ice in the sublimation front, [K]
T_s	Dried layer surface Temperature [K]
T_{af}	Air temperature in the batch freezer [^{o}C]
T_f	Initial freezing temperature of product, [^{o}C]
t	Time, [s]
t_{sp}	Duration of the sublimation period[s]
t_{dp}	Duration of the desorption period [s]
t_{fd}	Duration of the total freeze-drying process = t_{sp}+t_{dp} [s]
x_d	Dried layer thickness, [m]
Y	Fraction of residual ice content at time t defined in Equation (8), [dimensionless]
ρ_d	Dry matter density, [kg $_{drymatter}$ m^{-3}]
ρ_f	Frozen food density, [kg m^{-3}]

ucts such as pharmaceuticals and, more recently, some foods such as strawberry (Hammami & René, 1997; Shishehgarha et al., 2002), carrot, red pepper, mushroom (George & Datta, 2002), apple (Nakagawa & Ochiai, 2015) and banana (Wang et al., 2013).

However, despite the higher investment in equipment and greater processing costs, the cultural trend for convenience and product quality favors the production of freeze-dried foods. In fact, a US-based company (Harvest Right, LLC) already sells domestic freeze-dryers. Research on this subject, however, is still insufficient (Hammami & René, 1997), particularly in freeze-drying kinetics (Shishehgarha et al., 2002). The main challenge is to mathematically model freeze-drying of foods to gain a better understanding of the phenomenon as well as to cal-

culate process time and other design-related parameters. There are some relatively simple models to estimate sublimation time (Ratti, 2012) and water content as a function of time (Hua et al., 2010). Models usually consider heat being transferred by conduction from the bottom surface of samples while vapor exits through the top surface towards the vapor condenser. In this regard, George and Datta (2002) developed and validated a mathematical model of the heat and mass transfer for the primary drying stage of carrot slices. They neglected a mass transfer coefficient between the product surface and the condenser and concluded that the overall process rate is mass transfer-controlled. These authors also studied freeze-drying of mushroom and red pepper and found that pieces of the latter dried in about 5 h, with mushroom samples being slower to dry. In another configuration, heat influx through bottom and top surfaces is considered, so the relevant models differ. El-Maghlany et al. (2019) proposed a more complex analysis for the sublimation stage, considering the transfer mechanism through pores. These authors obtained satisfactory results but their study was limited only to the first step. Sadikoglu and Liapis (1997) developed mathematical expressions for the primary and secondary stages in their study of bulk solution freeze-drying where heat transfer was by conduction from the bottom surface and by radiation from the top surface, with mass transfer upwards and vapor exiting through the top surface. On the other hand, Alfat and Purqon (2017) studied the complete freeze-drying process, considering the transfer mechanism not only in the food but also with respect to the medium. These models are complex and must be solved by numerical methods. The literature paid less attention to intermediate-complexity models which improve the sublimation time classic model offered by Karel and Lund (2003), which only calculates the duration of the sublimation period for zero ice content. In fact, the primary drying period that encompasses sublimation along with the effect of the increasing dried layer thickness was seldom modelled to predict the water content as a function of time. Besides, modelling of the secondary drying, which proceeds by desorption and diffusion of vapor through the dried layer, involves a low proportion of the original water content but a considerable fraction of the total processing time, and deserves proper attention. On these grounds, the objective of this work was to mathematically model

1. the primary drying period, with an expression accounting for sublimation and the increasing dried layer to predict the curve of moisture content vs time, and

2. the secondary or desorption period, with an analytical solution of the unsteady state diffusion differential equation.

For this purpose, a well-founded limiting moisture content between the two stages was determined from a correlation and the study encompassed three fruits: apple, banana and strawberry.

2 Materials and Methods

2.1 Preparation of samples

Slices of peeled apple (*Malus domestica*) cv. Red Delicious), banana (*Musa Paradisiaca*) and strawberry (*Fragaria x Ananassa*) were prepared, though only one type of fruit was freeze-dried in each experiment. A device made of acrylic material was used to produce 0.01 m thick slices of fresh fruit by cutting them with a sharp knife. This thickness was employed throughout. Samples were placed on 0.3 m diameter trays. In turn, these trays were covered with food grade PVC film and introduced into a batch freezer, with air at -20 ^{o}C for 24 h. The tray cover avoided some dehydration that might occur during freezing and while the samples were moved from the freezer to the freeze-dryer chamber.

2.2 Equipment description

A Rificor model L-A-B4-C freeze dryer was used (RIFICOR, Buenos Aires, Argentina, http://www.rificor.com.ar/). The equipment consists of a cylindrical vacuum chamber made of transparent acrylic, covering a stainless-steel framework in which four disc-shaped shelves, spaced 0.07 m, are held. The shelves have built-in heating

elements and a Pt-100 temperature sensor connected to an automatic temperature controller up to 50 ^{o}C. Stainless steel trays (1 mm thick, 0.3 m diameter, with a lateral wall 0.02 m high), containing samples for freeze drying, are placed on the shelves. The equipment is fitted with a Pt-100 product temperature sensor, covered by a metallic case, and connected to a digital display. The chamber pressure was measured with a Pirani gauge, and the results continuously shown in a digital display. The equipment can be observed in Figures 1 and 2.

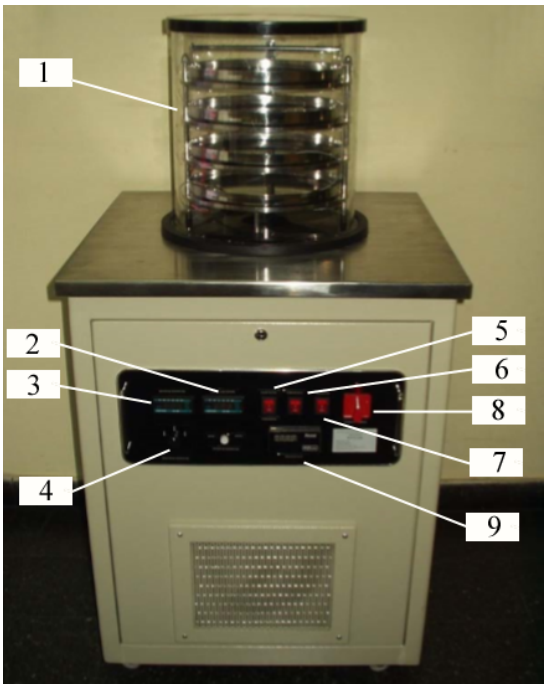

Figure 1: Rificor Freeze Dryer model L-A-B4-C. 1. Vacuum chamber; 2. Shelf temperature control; 3. Display showing either shelf, product or condenser temperature; 4. Switch to select the temperature being displayed 5. Switch that starts the condenser and its temperature measurement; 6. Switch for starting the vacuum pump and pressure gauge; 7. Switch to start heating the shelves; 8. Main switch; 9. Absolute pressure gauge.

Figure 2: Vacuum chamber of the Rificor L-A-B4-C Freeze dryer. 1. Tray; 2. Transparent vacuum chamber; 3. Temperature-controlled shelf; 4. Product temperature sensor; 5. Framework supporting the structure of the shelves under high vacuum.

2.3 Freeze-drying experiments

One tray with the frozen fruit was removed from the freezer, uncovered and placed in the freeze-dryer as the condenser temperature reached -48 ^{o}C. The cylindrical acrylic cover was put in place, and the vacuum pump was started. Chamber pressure was closely monitored and as soon as a value of 30 Pa was reached, shelf heating was switched on to set a target value of 40 ^{o}C. The saturation vapor pressure over ice at the freezing temperature is about 100 Pa, larger than the absolute pressure, and therefore much larger than the partial pressure of vapor remaining in the rarified atmosphere of the chamber thus avoiding ice melting. This last action was considered zero time for freeze-drying. To determine the experimental curve of moisture content as a function of time, triplicate experiments at 0, 1.5, 3, 4.5, 6, 8, 15, 19 and 24 h were carried out. Therefore, each experimental curve was built with 8 experiments

of different duration.
Moisture content for fresh and freeze-dried samples was determined in an Arcano (China) vacuum oven connected to a Vacuubrand PC 500 Series – CVC 3000 (Germany) diaphragm vacuum pump for 6 h at 70 ^{o}C, following the AOAC 934.06 method (AOAC International, 2016).

3 Results and Discussion

3.1 Theoretical considerations

Primary drying model: symmetrical heating from both sample surfaces

The slice of material (assumed a plane sheet) receives an inflow of heat by conduction from the shelf placed below the sample as well as heat by radiation from the upper shelf. This was inferred by observation of samples removed at early stages of preliminary freeze-drying tests: a dried layer of about the same size was observed above and below the frozen zone. Vapor, therefore, was considered to exit both through the bottom and top surfaces, and the characteristic length for vapor migration became half the initial sample thickness. Heat transfer was assumed symmetrical and so for the mass transfer rate. The scheme of mass and heat fluxes is shown in Figure 3.

The sublimation rate per unit area G, depends on the mass transfer as shown by Equation (1)

$$G = \frac{b}{x_d}(P_{iw} - P_{sw}) \tag{1}$$

Where x_d is the dried layer thickness, P_{iw} is the vapor pressure in the sublimation front and P_{sw} is the vapor pressure at the surface of the dried layer. Symbol b is the dried layer permeability to water vapor. In addition, the vapor transfer between the top surface and the condenser can be represented by:

$$G = k_g(P_{sw} - P_{aw}) \tag{2}$$

The symbol k_g stands for the mass transfer coefficient between the dried layer top surface and the condenser, which depends on equipment design and operating variables. The symbol, P_{aw} is the vapor pressure at the condenser temperature of -48 ^{o}C.

Ice temperature measured at the sublimation front were of -19, -18 and -22 ^{o}C for apple, banana, and strawberry, respectively. The vapor pressure of ice in the sublimation front was calculated by the following correlation published by Ratti (1991).

$$P_w = e^{(31.96 - \frac{6270.36}{T+273.15} - 0.461 \cdot ln(T+273.15))} \tag{3}$$

Using Equation (3), resulting values of P_{iw} for apple, banana and strawberry were 113.9, 125.2 and 85.3 Pa, respectively, for a P_{aw} of 5.0 Pa. As Equations (1) and (2) are different expressions for the same vapor flux, both can be equated as follows:

$$\frac{b}{x_d}(P_{iw} - P_{sw}) = k_g(P_{sw} - P_{aw}) \tag{4}$$

Although P_{iw} and P_{aw} keep constant in the primary drying period, P_{sw} becomes a function of the dry layer thickness x_d. By solving Equation (4) for P_{sw} we achieve the expression:

$$P_{sw} = \frac{bP_{iw} + k_g x_d P_{aw}}{x_d k_g + b} \tag{5}$$

This equation includes two parameters: b and k_g. By placing Equation (5) into Equation (2), and rearranging, the sublimation rate can be expressed in terms of the following flux equation:

$$G = \frac{P_{iw} - P_{aw}}{1/k_g + x_d/b} \tag{6}$$

Equation (6) predicts a time-varying vapor rate per unit area which is part of the transient macroscopic mass balance.
| Rate of accumulation of vapor inside the sample | = | Transfer rate through the dried layer, out of the sample and towards the condenser | The accumulation rate per unit area can be expressed as follows:

$$G = \rho_d \frac{L}{2}\frac{dm}{dt} \tag{7}$$

Where ρ_d is the density of the dry material and t is the instantaneous time. The negative sign must be written as dm/dt is inherently negative during dehydration. Where m stands for the moisture content, on a decimal dry basis, at time t. The model would be more general by

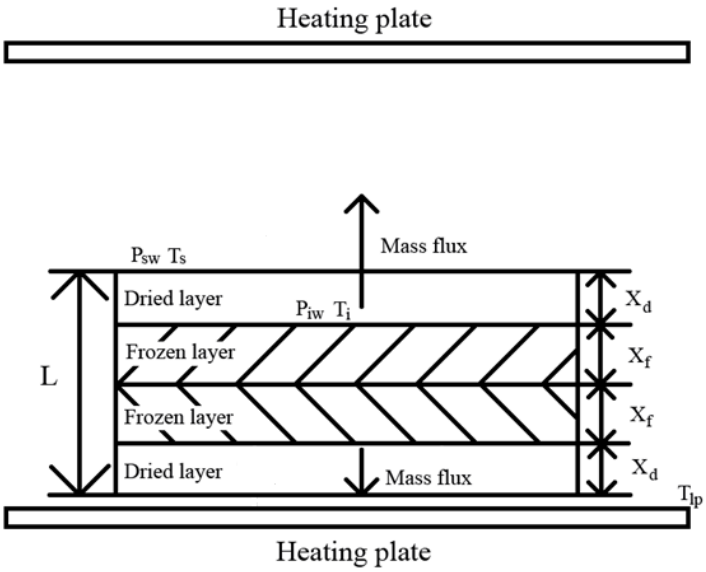

Figure 3: Schematic of freeze drying in the sample during the sublimation period.

normalizing the ratio of frozen water remaining (m - m_e) relative to the initial frozen water (m_0 - m_e) given by the expression:

$$Y = \frac{m - m_e}{m_0 - m_e} \tag{8}$$

Most models involving a dependent dimensionless variable would tend asymptotically to a limiting value, though that behavior is not expected for Y in the sublimation period, as m_e is not an equilibrium moisture content, but the maximum unfrozen water content for a freeze-dried fruit at the prevailing operating conditions. Therefore, experimental data should present a change in the drying mechanism (approximately for a time where $m \approx m_e$) from ice sublimation to water desorption.

By assuming uniform internal moisture distribution (a reasonable approximation in a sublimation front), the ratio of frozen water removed by sublimation relative to the initial frozen water content available for sublimation is 1-Y, which can be considered equivalent to the ratio of the dried layer thickness to the initial half thickness of the sample. This is represented by the following expression:

$$\frac{x_d}{L/2} = (1 - Y) \tag{9}$$

Where L is the sample thickness. Now, by differentiating Equation (8) with respect to time, a relationship is obtained between m and Y

$$\frac{dY}{dt} = \frac{dm}{dt}\frac{1}{(m_0 - m_e)} \tag{10}$$

Placing Equation (10) into Equation (7) and rearranging, the accumulation term becomes:

$$G = -\rho_d \frac{1}{2}(m_0 - m_e)\frac{dY}{dt} \tag{11}$$

The dry matter density is calculated from the value of the frozen food by assuming constant sample volume during the sublimation period, as shown in the equation below:

$$\rho_d = \frac{\rho_f}{1 + m_o} \tag{12}$$

Where ρf is the frozen food density. Now, by combining Equation (6) and (11):

$$-\rho_d \frac{L}{2}(m_0 - m_e)\frac{dY}{dt} = \frac{(P_{im} - P_{aw})}{1/k_g + x_d/b} \tag{13}$$

Now, by solving for x_d in Equation (9), placing it in Equation (13), and then multiplying both sides of the equal sign by 2/L and rearranging, the following expression is reached:

$$-\frac{dY}{dt}\frac{1-Y}{b}+\frac{2}{k_gL}=\frac{4(P_{iw}-P_{aw})}{L^2\rho_d(m_0-m_e)} \quad (14)$$

To simplify the writing, some variables kept constant during sublimation were grouped and termed C_{2m}:

$$C_{2m}=\frac{4(P_{iw}-P_{aw})}{L^2\rho_d(m_0-m_e)} \quad (15)$$

Multiplying both sides of Equation (15) by the dried layer permeability b:

$$-\frac{dY}{dt}((1-Y)+\frac{2b}{k_gL})=C_{2m}b \quad (16)$$

By integrating from Y=1 to a generic Y on the left-hand side, and from 0 to t on the right-hand side, we have:

$$\int_1^Y((1-Y)+\frac{2b}{k_gL})dY=-C_{2m}b\int_0^t dt \quad (17)$$

Multiplying both sides of the equation by (-2) and grouping part of the results in a binomial, an intermediate expression is found:

$$(1-Y)^2+\frac{4b}{k_gL}(1-Y)=2C_{2m}bt \quad (18)$$

With the purpose of grouping variables again in a binomial, the term (2b / (kg L))^2 is added at both sides of the equal sign to allow for the following equation:

$$\left(1-Y+\frac{2b}{k_gL}\right)^2=2C_{2m}bt+\left(\frac{2b}{k_gL}\right)^2 \quad (19)$$

By solving for Y, the first version of the model for the sublimation period is achieved:

$$Y=1+\frac{2b}{k_gL}-\sqrt{2C_{2m}bt+\left(\frac{2b}{k_gL}\right)^2} \quad (20)$$

To normalize experimental moisture contents (Equation (8)) to fit in Equation (20), the moisture content at the end of the sublimation period (m_e) is calculated from the fraction of unfrozen water in the previous freezing stage at -20 ^{o}C. This criterion is considered well-founded and original, and m_e does not only determine the endpoint of sublimation but also the starting point for the secondary period. To estimate the frozen water fraction, a correlation by Fikiin (1998), which is accurate for fruits, was employed:

$$F_{ice}=\frac{1.105}{1+\frac{0.7138}{ln(T_f-T_{af}+1)}} \quad (21)$$

Where F_{ice} is the fraction of frozen water in the sample, T_{af} is the air temperature in the freezer and T_f is the initial freezing temperature. Therefore, the fraction of unfrozen water, 1 – F_{ice}, can be used to calculate a delimiting moisture content between the primary and secondary drying periods.

$$m_e=m_0(1-F_{ice}) \quad (22)$$

Fitting of the sublimation model

Parameters and properties utilized here are listed in Table 1 (Choi & Okos, 1986; Quast & Karel, 1968). Experimental moisture contents and time were selected for the primary drying period, and moisture contents converted into the dimensionless variable Y as indicated by Equation (8), while Equation (20) was programmed in a user-defined MATLAB function. Equations and Figures were programmed and plotted in MATLAB 7.5.

Initial estimates for b and k_g were provided for the built-in function *nlinfit* to which the experimental data of Y vs t were supplied. The program thus written was able to determine the optimizing parameters b and k_g by nonlinear least squares, and the regression coefficient of determination, r^2. Fitted parameters for each fruit in this sublimation period are presented in Table 2. In Equation (20), two parameters of considerably different order of magnitude were obtained, and, although Table 2 shows that the expression provided accurate predictions, one must consider that the regression algorithm optimizes the parameters regardless of their physical meaning and in this sense, large variation for k_g, which makes it unreliable, and low variation for b were observed. Hence, by neglecting the external resistance to mass transfer, Equation (20) becomes:

$$Y=1-\sqrt{2C_{2m}bt} \quad (23)$$

Provided Equation (23) can maintain accurate predictions, more meaningful values of the dried layer permeability for each fruit might be determined. Fitted results of Equation (23) are presented in Table 3. A small loss of accuracy can be noticed only in apple but not in banana nor strawberry.
Now that the model has been simplified, C_{2m} can be expressed in its form of Equation (15), not to conceal the factors affecting the curve.

$$Y = 1 - \sqrt{\frac{8(P_{im} - P_{am})}{L^2 \rho_d (m_0 - m_e)} bt} \tag{24}$$

While the dried layer permeabilities, a kinetic parameter, are ordered from highest to lowest as strawberry > banana > apple, the plots of dimensionless Y vs dimensional t show the following order in drying rate: banana (fastest) > strawberry > apple (lowest). This behavior is probably due to the curve and is not explained solely by b. There are two consecutive steps: (1) sublimation of ice and (2) migration through the pores. Permeabilities explain migration but not sublimation, which can be described particularly by m_0-m_e, i.e., the mass of ice sublimed relative to the dry matter. Thus, a parameter called the sublimation kinetic coefficient k_s is defined:

$$k_s = \frac{8(P_{iw} - P_{aw})}{L^2 \rho_d (m_o - m_e)} b \tag{25}$$

This leads to the final form of the model for the sublimation period:

$$Y = 1 - \sqrt{k_s t} \tag{26}$$

Table 3 shows the values calculated for k_s. Ordering of this kinetic coefficient coincides with the order of sublimation rates of curves presented in Figure 4. Banana is less porous than strawberry though its mass of ice to sublime per kg of dry matter is also lower.
The values of b determined here for apple, banana and strawberry are comparable to the $3.5 \cdot 10^{-08}$ kg $_{water}$ (m Pa s)$^{-1}$ found by Quast and Karel (1968) in freeze-dried coffee. Values were also in the order of the $1.5 \cdot 10^{-08}$ kg $_{water}$ (m Pa s) $^{-1}$ published by Sandall et al. (1967) for turkey breast and $1.8 \cdot 10^{-08}$ kg $_{water}$ (m Pa s) $^{-1}$ as determined by Hill (1967) for beef.

Experimental data of Y vs t and predictions of the model in any of its equivalent forms (Equation (23), (24) or (26)), with the fitting parameter b for the sublimation period, are plotted in Figure 4. Calculated values follow the experimental behavior, and thus are substantially accurate for this difficult experimental system. Besides, the sublimation rate falls slightly (in absolute value) due to the influence of the increasing dried layer thickness during sublimation. This behavior was not clearly explained in the literature (Shishehgarha et al., 2002), which usually compares the sublimation period with the constant rate period that might be found in the convective drying of high-moisture foods, though the latter provides a linear behavior.

Secondary drying model

As the remaining unfrozen moisture is adsorbed on the food matrix, the vapor pressure will be lower than the value for the pure liquid at the same temperature. Some authors define this "state" as bound moisture. However, as the meaning of this concept is nebulous, we prefer to keep "adsorbed water". Then, adsorbed water must be desorbed and diffuse in the vapor state through the dried layer, exiting the sample towards the condenser. To model the secondary drying period an unsteady state mass balance was proposed, assuming the movement of vapor was governed by Fick's law of diffusion (Crank, 1975). The governing partial differential equation for a plane sheet is:

$$\frac{\partial m_l}{\partial t} = D \frac{\partial^2 m_l}{\partial x^2} \tag{27}$$

Where m_l stands for the local moisture content in the dried layer, now occupying the entire thickness of the sample, and D is the effective vapor diffusion coefficient. The initial and boundary conditions were:

$$t = 0 \qquad m_l = m_e \qquad 0 \leq x \leq L/2 \tag{28}$$

$$x = 0 \qquad \frac{\partial m_l}{\partial x} \qquad t > 0 \tag{29}$$

$$x = L/2 \qquad m_l = m_{eq} \qquad t > 0 \tag{30}$$

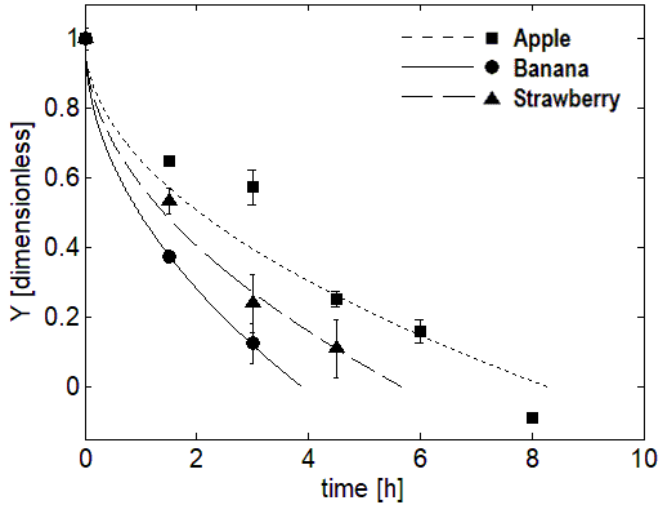

Figure 4: Experimental and predicted (Equation (26)) normalized moisture content ((m-me)/(m0-me)) as a function of time for the primary drying model. The standard deviations of data for apple, banana and strawberry are plotted as error bars.

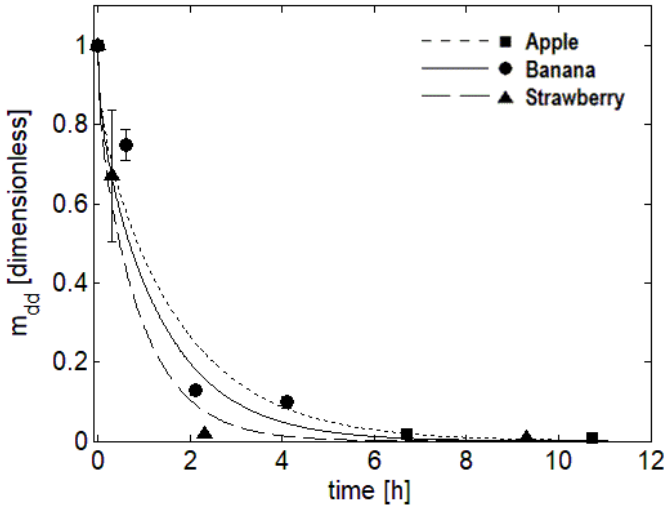

Figure 5: Dimensionless moisture content as a function of the desorption period time: apple (slower drying curve), banana (medium drying curve) and strawberry (faster drying curve). Values predicted by Eqs. (31) and (32) and experimental data with their respective standard deviations plotted as error bars.

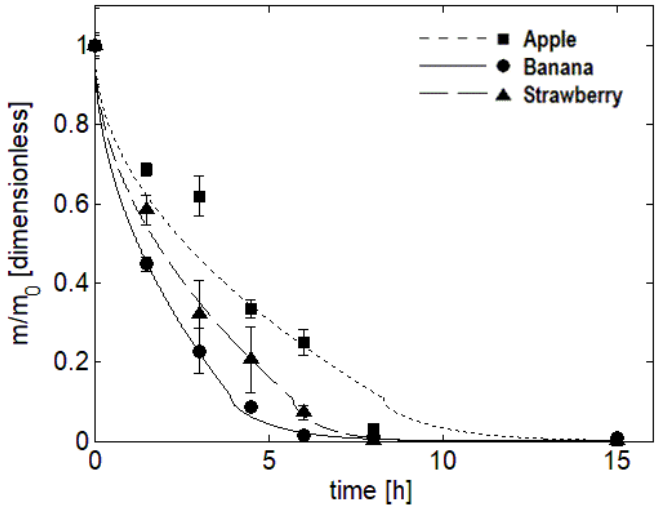

Figure 6: Normalized moisture content as a function of time for the complete freeze drying process: primary and secondary drying models. Values were predicted by Eqs. (26), (31) and (32). The standard deviations of data for apple, banana and strawberry are plotted as error bars.

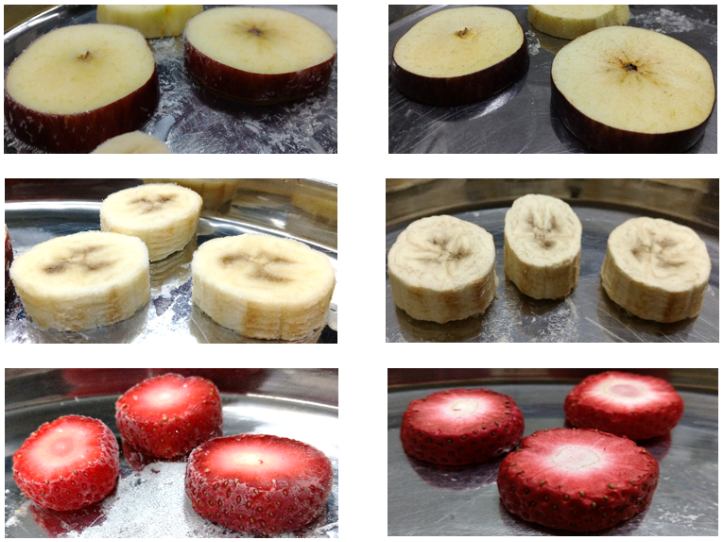

Figure 7: Frozen and freeze-dried pictures for apple, banana and strawberry: Left column for frozen fruits and Right column for freeze-dried products.

Table 1: Properties and operating conditions used to apply the sublimation drying model (Equation (21)) to the experimental data for the primary drying stage

	Apple	Banana	Strawberry
ρ_f (kg m^{-3})[a]	787	863	882
ρ_d (kg m^{-3})	116.79	214.73	88.02
m_0 (kg $_{water}$ kg $_{drymatter}$ $^{-1}$)	5.7386	3.0189	9.0208
m_e (kg $_{water}$ kg $_{drymatter}$ $^{-1}$)	0.6249	0.3529	0.9814
T_f (^{o}C)[b]	-1.45	-3.88	-1.39
T_{lp}(^{o}C)	40	40	40
L (m)	0.01	0.01	0.01
T_{af} (^{o}C)	-20	-20	-20
T_{iw} (^{o}C)	-19	-18	-22
P_{iw} (Pa)	113.9	125.3	85.3
P_{aw} (Pa)	5.0	5.0	5.0

[a] estimated by Choi and Okos (1986) equation.
[b] estimated from data published by Rahman (2008).

Table 2: Results for the primary drying period.

	Apple	Banana	Strawberry
Ice fraction during freezing (kg $_{ice}$ kg $_{initialwater}$ $^{-1}$)	0.8911	0.8831	0.8912
Duration of the sublimation period (h)	8.5 ± 0.26	4.0 ± 0.44	5.4 ± 0.58
Permeability b (kg $_{water}$ (m Pa s)$^{-1}$)	2.242E-09 ± 5.99E-11[a]	4.197E-09 ± 4.43E-10[b]	5.644E-09 ± 5.184E-10[c]
Convective mass transfer coefficient kg (kg water (m^2 Pa s)-1)	1.728E-06 ± 8.31E-7[d]	72.087 ± 18.936[e]	1.334E-05 ± 6.17E-6[f]
Coefficient of determination r^2	0.9799	0.9910	0.9532

[a,b,c] Average ± Standard Deviation (n=3) where different superscript letters on the same row are significantly different (α <0.05).
[d,e,f] Average ± Standard Deviation (n=3) where different superscript letters on the same row are significantly different (α <0.05).

Table 3: Results for the primary drying period by the simplified model (Eq (24))

	Apple	Banana	Strawberry
Ice fraction during freezing (kg $_{ice}$ kg $_{initialwater}^{-1}$)	0.891	0.883	0.891
Duration of the sublimation period (h)	8.5 ± 0.26	3.9 ± 0.34	5.5 ± 0.58
Permeability b (kg $_{water}$ (m Pa s)$^{-1}$)	2.433E-09 ± 6.020E-11^{a}	4.248E-09 ± 3.61E-10^{b}	5.538E-09 ± 5.166E-10^{c}
Sublimation kinetic coefficient k_s (s^{-1})	1.3087E-04 ± 4.1189E-6^{d}	2.8459E-04 ± 2.4620E-5^{e}	2.0193E-04 ± 2.1972E-5^{f}
Coefficient of determination r^2	0.9464	0.991	0.9502

^{a,b,c} Average ± Standard Deviation (n=3) where different superscript letters on the same row are significantly different (α <0.05).
^{d,e,f} Average ± Standard Deviation (n=3) where different superscript letters on the same row are significantly different (α <0.05).

Table 4: Results for the secondary drying period

	Apple	Banana	Strawberry
Diffusion coefficient (m^2 s^{-1})	1.628E-09 ± 2.554E-11^{a}	1.977E-09 ± 1.055E-9^{a}	2.285E-09 ± 2.213E-9^{a}
Coefficient of determination r^2	0.9999	0.9790	0.9762
Duration of the desorption stage (h)	4.3 ± 0.10	3.2 ± 1.35	3.3 ± 1.92
Duration of the freeze drying process (h)	12.8 ± 0.36	7.1 ± 1.11	8.9 ± 1.34

^{a} Average ± Standard Deviation (n=3) where different superscript letters on the same row are significantly different (α <0.05).

Table 5: Experimental values from the triplicate experiences with their respective standard deviation.

Process time [h]	Apple[a]	Banana[b]	Strawberry[c]
0	5.739 ± 0.182	3.019 ± 0.079	9.021 ± 0.871
1.5	3.943 ± 0.085	1.351 ± 0.052	5.283 ± 0.341
3	3.558 ± 0.289	0.687 ± 0.172	2.907 ± 0.758
4.5	1.917 ± 0.136	0.264 ± 0.014	1.865 ± 0.755
6	1.441 ± 0.187	0.045 ± 0.004	0.659 ± 0.164
8	0.174 ± 0.024	0.036 ± 0.005	0.016 ± 1.358E-03
15	1.116E-02 ± 2.418E-03	0.025 ± 3.911E-03	9.117E-03 ± 1.479E-03
19	6.029E-03 ± 1.169E-03	0.017 ± 7.097E-04	0.013 ± 3.251E-03
24	8.432E-03 ± 7.164E-04	0.012 ± 7.045E-05	8.729E-03 ± 1.164E-03

[a,b,c] Average ± Standard Deviation (n=3) where different superscript letters on the same row are significantly different (α <0.05). In order to improve the visualization of the Table, we omitted to place the superscripts over each value presented.

The time t is now counted from the start of the desorption period. The value of m_{eq} is the equilibrium moisture content at the operating conditions prevailing in the experiments, [kg $_{water}$ kg $^{-1}_{drymatter}$]. In the desorption period, and, because of the high vacuum conditions, this equilibrium value was assumed to be zero.

Assuming no shrinkage and constant volume (constant diffusion coefficient), Equation (27), together with the initial and boundary conditions expressed in Equations (28) to (30), can be integrated over the half volume of the sample. These assumptions are substantially met during desorption in a freeze-drying process. The analytical series solution is Crank (1975):

$$m_{dd} = \frac{8}{\pi^2} \sum_{n=0}^{\infty} \frac{1}{(2n+1)^2} e^{-\frac{(2n+1)^2 \pi^2 Dt}{4L^2}} \tag{31}$$

$$m_{dd} = \frac{m - m_{eq}}{m_e - m_{eq}} \tag{32}$$

Where m_{dd} is the dimensionless mean moisture content. As mentioned above, the starting moisture content in the desorption period (m_e) coincides with the final moisture content in the sublimation stage.

This combined equation was solved for the mean moisture content m for fitting to the experimental data of the secondary drying period, using a procedure already described for the sublimation period, but now to optimize parameter D. The moisture content-time data for the desorption period are not employed in the fitting of the sublimation model. The moisture content corresponding to the unfrozen water fraction, m_e is considered as a pseudo experimental point. For $m = m_e$, zero time was considered for the secondary drying. The duration of the primary period was previously calculated by the sublimation model as the time taken for moisture content to reduce from m_0 to m_e. Thus, the time used for fitting during the secondary period is the cumulative time minus the sublimation time. This is possible because the secondary drying period is assumed to start without a moisture content gradient through the thickness.

Equations (31) and (32) are written in a user-defined function file. The program module allows a variable number of terms to be employed, and the sum in Equation (31) is terminated for each time as the last term falls below 10^{-05}. With this adaptive programming, a lower number of terms are used towards the end of each fitting exercise. The optimized value of D and the goodness of fit parameters are presented in Table 4.

The coefficients of determination indicate that predictions in the secondary period were satis-

factory in general, being highly accurate in apple, accurate in banana and still very good in strawberry. All the calculations demanded only a few seconds of computing time which indicates the usefulness of the model for potential applications in control algorithms.

According to the theory of the glass transition, a critical moisture content must be defined to approach the glassy state of dry solid which results in a long-term stability of foods. For that reason, a final moisture content of 4% w/w or 0.0416 kg water kg dry matter^{-1} was used to calculate the secondary freeze-drying time. Some authors, who studied the glass transition phenomena in freeze-dried fruits, suggested a similar final moisture content which would be adequate for freeze-dried fruits' preservation at ambient temperature (Khalloufi & Ratti, 2003; Moraga et al., 2011; Mosquera et al., 2012). The total freeze-drying time is shown in Equation (33):

$$t_{fd} = t_{sp} + t_{dp} \tag{33}$$

Where t_{dp} is the duration of desorption period, t_{fd} is the length of the total freeze-drying process and t_{sp} stands for the duration of the sublimation period, all times being in s.

Predictions of the model were in fair agreement with the experimental m_{dd} as a function of time as observed in Figure 5 for the three fruits. Times were converted to h in the graph for easier visualization.

In Figure 4, the ordering of curves follows the same ordering of the sublimation kinetic coefficient k_s because, as mentioned above, it depends not only on permeability b but also on the amount of ice being sublimed relative to the dry matter. In contrast, in Figure 5, the ordering of curves occurs in the same mode as the ordering of the vapor diffusion coefficients because in the latter period the sole relevant mass transfer parameter is D. This is related to the structure and its porosity.

As moisture content at the end of the process is low and, in relative terms, is more affected by errors than values in the sublimation period, triplicate experiments are particularly useful in the desorption period and especially towards the end of it.

The diffusion coefficient determined here in apple was somewhat higher than that reported by Saravacos (1967) in the same freeze-dried fruit, $0.7 \cdot 10^{-09}$ m^2 s^{-1}, because the shelf temperature was 40 ^{o}C here compared with 30 ^{o}C in the author's study. In turn, the diffusivity for air-dried banana slices at 38 ^{o}C was $2.1 \cdot 10^{-10}$ m^2 s^{-1} which is much lower than the diffusivity for banana found in this work. On the other hand, atmospheric pressure tends to increase the diffusion coefficient but the collapsed structure of an air-dried fruit reduces this parameter markedly (Saha et al., 2018). No diffusion coefficients during freeze drying studies were found for strawberry. Interestingly, as observed in Tables 3 and 4, the ordering of permeabilities in the sublimation period coincides with the ordering of diffusion coefficients in the desorption stage (apple<banana<strawberry). This is consistent with the nature of b and D, which is related to the movement of water vapor through the porous structure of the dried layer.

Tables 3 and 4 show the most representative permeabilities and diffusion coefficients for the primary and secondary drying periods, respectively. A statistical study of analysis of variance was performed (α=0.05) to find out if the difference between the parameters obtained is significant or not. Regarding the permeability, the results showed that there was a significant difference among the values obtained for each fruit. This can be related to difference in their structure, their chemical composition and initial moisture content. These factors affect the dried layer thickness and the amount of ice per kg of dry matter and therefore impact directly on the value of b for each fruit. On the other hand, there is no significant difference between the diffusion coefficients which may be associated with the complete sublimation of ice and the movement of remaining water through the pores of the dry matter during this period. In this situation, where the moisture content is so low, it is reasonable to assume that the diffusion coefficient does not show significant differences.

Predictions of both models adapted for the moisture content dry basis, normalized by the initial moisture content as a function of time, together with the experimental data for the two periods (Equations (8), (26), (31) and (32)) are plotted in Figure 6.

In Figure 6 predictions are observed to follow the

experimental behavior substantially well. The transition between predictions of models for the primary and secondary periods can be identified by a change of slope. Continuity of moisture content between the models was ensured but not in the derivatives due to the diverse drying mechanisms in the two periods.
Finally, in Figure 7, some images of each fruit, before and after the freeze drying process are presented. As can be seen, there is little difference between the initial and final appearance for the fruits, which is one of the more attractive results of this drying methodology.

4 Conclusions

A well-founded model was developed for the sublimation drying of fruits with symmetrical mass transfer, considering the increasing dried layer to predict the remaining ice content relative to the original. The model was fitted to experimental data for apple, banana and strawberry to provide an accurate representation of the observed behavior. Dried layer permeabilities (b) were determined to be 2.3 to $5.4 \cdot 10^{-09}$ kg $_{water}$ (m Pa s)$^{-1}$, though the relevant kinetic parameter was a combination of b and the mass of sublimed ice relative to the dry matter, whose ordering was congruent with the arrangement or experimental sublimation rates. Another original feature was the use of the moisture content corresponding to the unfrozen water fraction as a limit between primary and secondary periods. A falling sublimation rate was observed and predicted for the three fruits which was caused by the increasing dried layer thickness.
The secondary drying was modelled with the analytical solution of the diffusion equation. Predictions were accurate for this low moisture content period, and allowed effective diffusion coefficients, in high vacuum, to be in the range of 1.6 to $2.9 \cdot 10^{-09}$ m^2 s^{-1}. These values are one to two orders of magnitude higher than values reported in the literature for the convective drying of fruits at atmospheric pressure. Although, the secondary drying period takes place at high vacuum, a factor that is known to reduce the diffusion coefficient, suggests the creation of a porous structure. The ordering of D in the three fruits was representative for the desorption rates in this period and coincides with the ordering of permeabilities in the sublimation period, as both parameters represent the migration of vapor through the porous structure.
In general, this two-model approach to simulate freeze drying of fruits was fairly accurate, well founded and demanded short computing time, making it suitable for use within an application as an interactive tool for freeze-dryer design and even, as part of fast-response automatic control algorithms.

References

Alfat, S., & Purqon, A. (2017). Heat and mass transfer model in freeze-dried medium. *Journal of Physics: Conference Series*, *877*, Article 012061. https://doi.org/10.1088/1742-6596/877/1/012061

AOAC International. (2016). AOAC official method: 934.06 moisture in dried fruits. In G. W. Latimer (Ed.), *Official methods of analysis of AOAC International*.

Choi, Y., & Okos, M. R. (1986). Effects of temperature and composition on the thermal properties of foods. In M. Le Maguer & P. Jelen (Eds.), *Food engineering and process applications* (pp. 93–101, Vol. 1). Elsevier.

Crank, J. (1975). *The mathematics of diffusion* [OCLC: 1320797]. Clarendon Press.

El-Maghlany, W. M., Bedir, A. E.-R., Elhelw, M., & Attia, A. (2019). Freeze-drying modeling via multi-phase porous media transport model. *International Journal of Thermal Sciences*, *135*, 509–522. https://doi.org/10.1016/j.ijthermalsci.2018.10.001

Fikiin, K. A. (1998). Ice content prediction methods during food freezing: A survey of the Eastern European literature. *Journal of Food Engineering*, *38*(3), 331–339. https://doi.org/10.1016/S0260-8774(98)00120-4

García-Amezquita, L. E., Welti-Chanes, J., Vergara-Balderas, F. T., & Bermúdez-Aguirre, D. (2016). Freeze-drying: The basic process. In B. Caballero, P. M. Fin-

glas, & F. Toldrá (Eds.), *Encyclopedia of food and health* (pp. 104–109). Academic Press. https://doi.org/10.1016/B978-0-12-384947-2.00328-7

George, J. P., & Datta, A. K. (2002). Development and validation of heat and mass transfer models for freeze-drying of vegetable slices. *Journal of Food Engineering*, *52*(1), 89–93. https://doi.org/10.1016/S0260-8774(01)00091-7

Hammami, C., & René, F. (1997). Determination of freeze-drying process variables for strawberries. *Journal of Food Engineering*, *32*(2), 133–154. https://doi.org/10.1016/S0260-8774(97)00023-X

Hill, J. E. (1967). *Sublimation dehydration in the continuum, transition, and free-molecule flow regimes* [Doctoral dissertation]. Georgia Institute of Technology. Retrieved February 3, 2023, from http://hdl.handle.net/1853/16723

Hua, T.-C., Liu, B.-L., & Zhang, H. (2010). *Freeze-drying of pharmaceutical and food products*. Woodhead Publishing. Literaturverz. S. [242] - 249.

Karel, M., & Lund, D. B. (2003). *Physical principles of food preservation* (2nd ed.) [OCLC: 473941727]. Marcel Dekker.

Khalloufi, S., & Ratti, C. (2003). Quality deterioration of freeze-dried foods as explained by their glass transition temperature and internal structure. *Journal of Food Science*, *68*(3), 892–903. https://doi.org/10.1111/j.1365-2621.2003.tb08262.x

Moraga, G., Talens, P., Moraga, M. J., & Martínez-Navarrete, N. (2011). Implication of water activity and glass transition on the mechanical and optical properties of freeze-dried apple and banana slices. *Journal of Food Engineering*, *106*(3), 212–219. https://doi.org/10.1016/j.jfoodeng.2011.05.009

Mosquera, L. H., Moraga, G., & Martínez-Navarrete, N. (2012). Critical water activity and critical water content of freeze-dried strawberry powder as affected by maltodextrin and Arabic gum. *Food Research International*, *47*(2), 201–206. https://doi.org/10.1016/j.foodres.2011.05.019

Nakagawa, K., & Ochiai, T. (2015). A mathematical model of multi-dimensional freeze-drying for food products. *Journal of Food Engineering*, *161*, 55–67. https://doi.org/10.1016/j.jfoodeng.2015.03.033

Quast, D. G., & Karel, M. (1968). Dry layer permeability and freeze-drying rates in concentrated fluid systems. *Journal of Food Science*, *33*(2), 170–175. https://doi.org/10.1111/j.1365-2621.1968.tb01344.x

Ratti, C. (1991). *Diseño de secaderos de productos frutihortícolas* [Doctoral dissertation]. Universidad Nacional del Sur.

Ratti, C. (2012). Freeze-drying process design [Section: 22]. In J. Ahmed & M. S. Rahman (Eds.), *Handbook of food process design* (pp. 621–647). John Wiley & Sons. https://doi.org/10.1002/9781444398274.ch22

Sadikoglu, H., & Liapis, A. I. (1997). Mathematical modelling of the primary and secondary drying stages of bulk solution freeze-drying in trays: Parameter estimation and model discrimination by comparison of theoretical results with experimental data. *Drying Technology*, *15*(3-4), 791–810. https://doi.org/10.1080/07373939708917262

Saha, B., Bucknall, M., Arcot, J., & Driscoll, R. (2018). Derivation of two layer drying model with shrinkage and analysis of volatile depletion during drying of banana. *Journal of Food Engineering*, *226*, 42–52. https://doi.org/10.1016/j.jfoodeng.2018.01.010

Sandall, O. C., King, C. J., & Wilke, C. R. (1967). The relationship between transport properties and rates of freeze-drying of poultry meat. *AIChE Journal*, *13*(3), 428–438. https://doi.org/10.1002/aic.690130309

Saravacos, G. D. (1967). Effect of the drying method on the water sorption of dehydrated apple and potato. *Journal of Food Science*, *32*(1), 81–84. https://doi.org/10.1111/j.1365-2621.1967.tb01963.x

Shishehgarha, F., Makhlouf, J., & Ratti, C. (2002). Freeze-drying characteristics of

strawberries. *Drying Technology*, *20*(1), 131–145. https://doi.org/10.1081/DRT-120001370

Wang, H.-Y., Zhang, S.-Z., Yu, X.-Y., & Chen, G.-M. (2013). Water vapor diffusion coefficient of freeze-dried banana slices. *Food Science*, *34*, 66–70.